Manuscript submitted to
AIMS' Journals
Volume **X**, Number **0X**, XX **200X**

Website: http://AIMsciences.org

pp. **X–XX**

A WASSERSTEIN APPROACH TO THE NUMERICAL SOLUTION OF THE ONE-DIMENSIONAL CAHN-HILLIARD EQUATION

Fausto Cavalli

Università degli Studi di Brescia
Dipartimento di Matematica
Via Valotti 9, 25133 Brescia (Italy)

Giovanni Naldi

Università degli Studi di Milano
Dipartimento di Matematica "F. Enriques"
Via Saldini 50, 20133 Milano (Italy)

Abstract. In this work we introduce a numerical approach for solving Cahn-Hilliard equation with Neumann boundary conditions involving recent mass transportation methods. The numerical scheme is based of an alternative formulation of the problem using the pseudo-inverse of the a suitable cumulative distribution function. We establish a stable fully discrete schemes that inherit the energy dissipation property and mass conservation property from the associated continuous problem. We perform some numerical experiments which confirm our results.

1. **Introduction.** When a mixture of two metallic components is heated, and then rapidly cooled to a lower temperature, a sudden phase separation can occur. This separation of the metal alloy into two components, via cooling, is called spinodal decomposition. Understanding the process of this segregation, as well as finding any steady states that may remain after cooling has been the subject of much research (see for example [1] and reference therein). One of the first chemical model and on the spinodal decomposition problem is introduced in late 1950s [2, 3, 4, 5, 6] by John Cahn and John Hilliard. They proposed a chemical model that has the following energy (in the one-dimensional case),

$$E(u) = \int \left(\phi(u) + \kappa(\partial_x u)^2\right) dx,$$

where $\phi(u)$ is the free-energy density of the material $u(x,t)$, and $\kappa(\partial_x u)^2$ is the additional free-energy density if the material is in a gradient in composition (i.e., in a transition between two states). Additionally, mass is assumed to be conserved in this system, giving

$$\int u(x,t)dx = m.$$

2000 *Mathematics Subject Classification.* Primary: 65M06, 65M12; Secondary: 35Q70.

Key words and phrases. Cahn-Hilliard equation; pseudo-inverse function; stable numerical methods for fourth order equations.

This work was partially supported by national PRIN2007 project "Modellistica numerica per il calcolo scientifico ed applicazioni avanzate".

Usually, the Neumann boundary conditions are chosen to prohibit the flow of material into or out of the confined volume,

$$\partial_x u = \partial_x \left(\phi(u) + \kappa (\partial_x u)^2 \right) = 0,$$

which is possible to simplify since $\partial_x \phi(u) = \phi'(u) \partial_x u$, then

$$\partial_x u = \partial_{xxx} u = 0.$$

The Cahn-Hilliard model was originally derived using chemical and physical principles to describe the phase separation process. However, an alternative deduction as a gradient flow is possible as has been shown by Fife [1] by considering the spinodal decomposition of a two-phase system will minimize the following energy $\mathcal{F}$ (here for the one dimensional case),

$$\mathcal{F}[u] \equiv \int \left[W(u(x)) + \frac{1}{2} \epsilon^2 |\partial_x u|^2 \right] dx, \tag{1}$$

where ϵ is a small positive parameter and $W(u)$ is any "double well potential" ($W(u)$ is smooth, has two local minima and has only one local maximum between them). Then it is natural to seek a law of evolution in the form

$$\partial_t u = -\alpha \nabla_c \mathcal{F}[u], \tag{2}$$

for some positive constant or function α and where ∇_c here denotes a constrained gradient in some Hilbert space. Following the discussion in [1] it is possible to achieve the law of motion

$$\partial_t u = \alpha \partial_{xx} \left[W'(u) - \epsilon^2 \partial_{xx} u \right], \tag{3}$$

which is the Cahn Hilliard equation when α is chosen to be a constant.

By exploiting the gradient flow structure of the Cahn-Hilliard equation it is possible to point out similarities between this equation and the second order equations. Moreover it suggests to consider the point of view of optimal transportation and the use of the techniques related with it [].

The scheme is natural in the sense that it relies on the gradient flow structure of the problem as we will see in the following subsection.

$$u_t = (\phi(u) + q u_{xx})_{xx} \tag{4}$$

with initial datum

$$u(x,t) = u_0(x) \tag{5}$$

where $\phi(u) = \Phi'(u)$ and the potential $\Phi(u)$ has the form

$$\Phi(u) = \frac{1}{2}(u^2 - 1)^2 \tag{6}$$

$(u - c_2)(u - c_1)(2u - c_2 - c_1)$ and $q < 0$. The boundary conditions are

$$\begin{aligned} \left. \frac{\partial u}{\partial x} \right|_a &= \left. \frac{\partial u}{\partial x} \right|_b = 0 \\ \left. \frac{\partial \phi(u) + q u_{xx}}{\partial x} \right|_a &= \left. \frac{\partial \phi(u) + q u_{xx}}{\partial x} \right|_b = 0 \end{aligned} \tag{7}$$

For equation (4) there are two important properties: the mass conservation

$$\frac{d}{dt} \int_a^b u(x,t) dx = 0 \tag{8}$$

and the energy dissipation

$$\frac{d}{dt}\int_a^b G(u(x,t))dx \leq 0 \tag{9}$$

2. **Pseudo-inverse formulation.** The derivation of the numerical scheme passes through the reformulation of (4) in terms of the pseudo-inverse of the integral function of u. The following description follows the apporach used in [**?**].

First we introduce the function $F_0 : [a,b] \to [0,m]$

$$F_0(x) = \int_a^x u_0(y)dy \; x \in [a,b] \tag{10}$$

where $m = \int_a^b u_0(y)dt$; in the particular case of $m = 1$ we have that $u_0(x)$ can be associated to a probability density and $F_0(x)$ is the associated distribution function. Equation (4) has an equivalent formulation in the sense of distribution functions as

$$\partial_t F = \partial_x \phi(\partial_x F) + q\partial_{xxxx} F, \quad F(x,0) = F_0(x), \tag{11}$$

from which we can deduce the relation

$$u = \partial_x F. \tag{12}$$

Due to the positivity of $u_0(x)$, the function $F_0(x)$ is non-decreasing and so we can define its pseudo-inverse function $x_0 : [0,m] \to [a,b]$

$$x_0(\rho) = \inf\{x : F_0(x) = \rho\}.$$

Now we can define $X : [0,m] \times [0,T] \to [a,b]$ using the implicit function theorem as the reciprocal mapping of the solution $F(x,t)$ of the equation (11)

$$F(X(\rho,t),t) = \rho \tag{13}$$

provided that $\partial_x \rho \neq 0$.

Finally we can deduce a time evolution equation for $X(\rho,t)$ from (11): to perform this we make use of the following

Lemma 2.1. *Let $u(x,t) : [a,b] \times [0,T] \to \mathbb{R}$ be a non negative sufficiently regular function which satisfies equation (4) and define its pseudo-inverse function $X(\rho,t)$. Define also the following operator T_ρ as*

$$T_\rho(\cdot) = \frac{1}{\partial_\rho X}\partial_\rho(\cdot).$$

Then the following relations are valid:

$$\partial_t X(\rho,t) = -\left.\frac{1}{u(x,t)}\partial_t F(x,t)\right|_{x=X(\rho,t)}, \tag{14a}$$

$$\left.\partial_x^{(n)} u(x,t)\right|_{x=X(\rho,t)} = T_\rho^n\left(\frac{1}{\partial_\rho X(\rho,t)}\right) \quad n \geq 1. \tag{14b}$$

In particular we have

$$\left.\partial_x u(x,t)\right|_{x=X(\rho,t)} = \frac{1}{2}\partial_\rho\left(\frac{1}{\partial_\rho X^2}\right), \tag{14c}$$

$$\left.\partial_{xxx} u(x,t)\right|_{x=X(\rho,t)} = \frac{1}{2}\frac{1}{\partial_\rho X}\partial_\rho\left(\frac{1}{\partial_\rho X}\partial_{\rho\rho}\left(\frac{1}{\partial_\rho X^2}\right)\right). \tag{14d}$$

Proof. We notice that that, thanks to the definition (13) of X , we have

$$\frac{dF}{dt} = \partial_t F + \partial_x F \partial_t X = 0,$$

from which the first relation (14a) can be immediatly derived. To prove (14b) we proceed by induction: when $n = 0$ we need to show that

$$u(x,t)\Big|_{x=X(\rho,t)} = \frac{1}{\partial_\rho X(\rho,t)},$$

which is a straightforward consequence of the derivation rule for inverse functions, i.e.

$$\partial_\rho X(\rho,t) = \frac{1}{\partial_x F(x,t)}\Big|_{x=X(\rho,t)} = \frac{1}{u(X(\rho,t),t)}.$$

Now suppose that (14b) is valid for n : then we can compute

$$\partial_\rho \partial_x^{(n)} u(x,t)\Big|_{x=X(\rho,t)} = \partial_\rho T_\rho^n \left(\frac{1}{\partial_\rho X(\rho,t)}\right),$$

and

$$\partial_\rho \partial_x^{(n)} u(x,t)\Big|_{x=X(\rho,t)} = \partial_x^{(n+1)} u(x,t)\Big|_{x=X(\rho,t)} \partial_\rho X(\rho,t).$$

Equating the two left hand sides of the previous equations we have that the relation (14b) is valid for $n+1$. Moreover since

$$\frac{1}{\partial_\rho X}\partial_\rho \left(\frac{1}{\partial_\rho X}\right) = \frac{1}{2}\partial_\rho \left(\frac{1}{\partial_\rho X^2}\right),$$

we obtain (14c) and (14d). □

Now we are able to perform the change of variable in (4): the resulting evolution equation for $X(\rho,t)$ is

$$X_t = -\partial_\rho \left(\phi\left(\frac{1}{\partial_\rho X}\right) + \frac{1}{2}\frac{q}{\partial_\rho X}\partial_{\rho\rho}\left(\frac{1}{\partial_\rho X^2}\right)\right), \tag{15a}$$

with the initial condition defined by the pseudo inverse of the function F_0

$$X_0(\rho) = F_0^{-1}(\rho) = \inf\{x : F_0(x) = \rho\}. \tag{15b}$$

To complete the formulation of the problem in term of the pseudo inverse we must specify suitable boundary conditions: a natural choiche consists in rewriting in terms of the new variables the orginal boundary conditions (7) imposed on the Cahn-Hilliard equation (4), obtaining

$$\begin{aligned}
&\partial_\rho \left(\frac{1}{\partial_\rho X^2}\right) = 0 && \text{for } \rho = 0, m,\\
&\frac{1}{\partial_\rho X}\partial_\rho \left(\phi\left(\frac{1}{\partial_\rho X}\right) + \frac{1}{2}\frac{q}{\partial_\rho X}\partial_{\rho\rho}\left(\frac{1}{\partial_\rho X^2}\right)\right) = 0 && \text{for } \rho = 0, m.
\end{aligned}$$

It is easy to see that they are equivalent to

$$\partial_{\rho\rho} X = 0 \text{ for } \rho = 0, m, \tag{16a}$$

$$\partial_t X \text{ for } \rho = 0, m, \tag{16b}$$

where we used $\partial_\rho X \neq 0$, which is a straight consequence of the non negativity of u. Conditions (16) actually suggests that the original boundary conditions for the variable u (7) translate into to a Dirichlet boundary condition (16b) and a second order homogeneus Neumann boundary condition (16a).

The original differential problem is so replaced by equation (15), which is solved and $X(\rho,t)$ is retrieved; then, if needed, the solution u of the equation (4) can be easily reconstructed, defining the function F through the relation (13) and then deducing u from the identity (12).

In section 1 we introduced two important properties satisfied by equation (4), the mass conservation (8) and the energy dissipation (9): now we look for analogous properties for the new equation (15a). The conservation of the mass is a straightforward consequence of the pseudo-inverse formulation: the mass m of the original variable u is represented through the cumulative mass variable $F(t,b)$, which does not depend on time. For the dissipation of the energy we have the following

Theorem 2.2. *Consider the solution $X(\rho,t)$ of the Cauchy problem (15) associated with the non negative boundary conditions (16) and let us introduce the following energy functional*

$$G(\partial_\rho X) = \Gamma(\partial_\rho X) - \frac{q}{2}\frac{1}{\partial_\rho X}\partial_\rho\left(\frac{1}{\partial_\rho X}\right)^2,$$

where

$$\Gamma(u) = u\Phi(u^{-1}),$$

If we define the total energy as

$$E(t) = \int_0^m G(\partial_\rho X)d\rho, \tag{17}$$

then we have the following energy dissipation property

$$\frac{d}{dt}E(t) \le 0. \tag{18}$$

Proof. To prove the inequality (18) we consider separately

$$E_1(\partial_\rho X) = \Gamma(\partial_\rho X)$$

and

$$E_2(\partial_\rho X) = -\frac{q}{2\partial_\rho X}\partial_\rho\left(\frac{1}{\partial_\rho X}\right)^2.$$

For the first term we have

$$\begin{aligned}\frac{d}{dt}\int_0^m E_1(\partial_\rho X)d\rho &= \int_0^m E_1'(\partial_\rho X)\partial_{\rho t}X d\rho \\ &= -\int_0^m \partial_\rho\left(E_1'(\partial_\rho X)\right)\partial_t X d\rho \\ &\quad +\Big[E_1'(\partial_\rho X)\partial_t X\Big]_{\rho=0}^m,\end{aligned} \tag{19}$$

where the last term is null due to the boundary condition (16b). For the second term we can write

$$\begin{aligned}\frac{d}{dt}\int_0^m E_2(\partial_\rho X)d\rho &= -\frac{q}{2}\frac{d}{dt}\int_0^m \frac{\partial_\rho^2 X^2}{\partial_\rho X^5}d\rho \\ &= -\frac{q}{2}\frac{d}{dt}\int_0^m \left(\frac{2}{3\partial_\rho X^{3/2}}\right)_\rho^2 d\rho \\ &= -q\int_0^m \partial_\rho\left(\frac{2}{3\partial_\rho X^{3/2}}\right)\partial_{\rho t}\left(\frac{2}{3X_\rho^{3/2}}\right)d\rho.\end{aligned}$$

Integrating by parts the last expression we have

$$\begin{aligned}\frac{d}{dt}\int_0^m E_2(\partial_\rho X)d\rho &= q\int_0^m \partial_{\rho\rho}\left(\frac{2}{3\partial_\rho X^{3/2}}\right)\partial_t\left(\frac{2}{3\partial_\rho X^{3/2}}\right)d\rho \\ &\quad -\left[\partial_\rho\left(\frac{2}{3\partial_\rho X^{3/2}}\right)\partial_t\left(\frac{2}{3\partial_\rho X^{3/2}}\right)\right]_{\rho=0}^{m},\end{aligned}$$

where the last term is null thanks to (16a) since we have

$$\partial_\rho\left(\frac{2}{3\partial_\rho X^{3/2}}\right)\partial_t\left(\frac{2}{3\partial_\rho X^{3/2}}\right) = \frac{2}{\partial_\rho X^3}\partial_{\rho\rho}X\partial_{\rho t}X.$$

Going on we can write

$$\begin{aligned}\frac{d}{dt}\int_0^m E_2(\partial_\rho X)d\rho &= q\int_0^m \partial_{\rho\rho}\left(\frac{2}{3\partial_\rho X^{3/2}}\right)\partial_t\left(\frac{2}{3\partial_\rho X^{3/2}}\right)d\rho \\ &= -q\int_0^m \partial_{\rho\rho}\left(\frac{2}{3\partial_\rho X^{3/2}}\right)\left(\frac{1}{\partial_\rho X^{5/2}}\right)\partial_{\rho t}X d\rho \\ &= +q\int_0^m \partial_\rho\left(\partial_{\rho\rho}\left(\frac{2}{3\partial_\rho X^{3/2}}\right)\left(\frac{1}{\partial_\rho X^{5/2}}\right)\right)\partial_t X d\rho \\ &\quad -\left[\partial_{\rho\rho}\left(\frac{2}{3\partial_\rho X^{3/2}}\right)\partial_t X\right]_{\rho=0}^{m},\end{aligned} \tag{20}$$

where again the last term is null due to the boundary condition (16b). Summing the final identities in (19) and (20) we have

$$\begin{aligned}\frac{d}{dt}\int_0^m G(\partial_\rho X)d\rho &= \int_0^m\Bigg[-\partial_\rho\left(E_1'(\partial_\rho X)\right) \\ &\quad +q\partial_\rho\left(\partial_{\rho\rho}\left(\frac{2}{3\partial_\rho X^{3/2}}\right)\left(\frac{1}{\partial_\rho X^{5/2}}\right)\right)\Bigg]\partial_t X d\rho.\end{aligned} \tag{21}$$

Simple computations show that

$$\partial_\rho(\Gamma'(\partial_\rho X)) = -\frac{1}{\partial_\rho X}\partial_\rho\left(G'\left(\frac{1}{\partial_\rho X}\right)\right)$$

and

$$\partial_\rho\left(\partial_{\rho\rho}\left(\frac{2}{3\partial_\rho X^{3/2}}\right)\left(\frac{1}{\partial_\rho X^{5/2}}\right)\right) = \frac{1}{\partial_\rho X}\partial_\rho\left(\frac{1}{\partial_\rho X}\partial_{\rho\rho}\left(\frac{1}{2\partial_\rho X^2}\right)\right)$$

so, using in (21) the expression of X_t and noting that the non negativity of u implies $\partial_\rho X \geq 0$, we can conclude that (18) is true. □

3. **Numerical scheme.** To derive a numerical approximation for the solution u of (4) we proceed by discretizing equation (15a) and evolving in time $X(\rho,t)$; we remark that we do not have to recontruct at each time step the solution $u(X(\rho,t),t)$. However, to preserve the physical meaning and the origin of $X(\rho,t)$ we must take care that the scheme we propose be monotonicity preserving, to grant the solvability of (13).

We start introducing the spatial discretization for the variable $\rho \in [0,m]$ in the following way: we set $N+1$ equally spaced points $x_k \in [a,b]$ given by $x_k = a+k\Delta x$, for $k = 0,\dots,N$, where $\Delta x = (b-a)/N$, then we choose $\rho_k = F_0(x_k)$. We also define $\rho_{k+1/2} = F_0(x_{k+1/2})$, where $x_{k+1/2} = a+(k+1/2)\Delta x$ are the midpoints of the grid $[x_k, x_{k+1}]$. Then we introduce a time integration step $\Delta t > 0$ and we define

$t^n = n\Delta t, n \geq 0$; finally X_k^n is the approximation of $X(\rho_k, t^n)$. We emphasize that, thanks to (13), we have

$$F(X_k^n, t^n) = \rho_k \quad \forall n,$$

and so ρ_k is constant in time.

The scheme we propose for (15a) is then the following:

$$\begin{aligned} X_k^{n+1} =& X_k^n - \frac{\Delta t}{\rho_{k+1/2} - \rho_{k-1/2}} \left(\phi\left(\frac{\rho_{k+1} - \rho_k}{X_{k+1}^n - X_k^n} \right) - \phi\left(\frac{\rho_k - \rho_{k-1}}{X_k^n - X_{k-1}^n} \right) \right) \\ & - \frac{q\Delta t}{2(\rho_{k+1/2} - \rho_{k-1/2})} \left(\Psi_{k+1/2}^n - \Psi_{k-1/2}^n \right), \end{aligned} \tag{22}$$

where

$$\begin{aligned} \Psi_{k+1/2}^n = \Bigg(& \frac{\rho_{k+1} - \rho_k}{X_{k+1}^n - X_k^n} \frac{\left(\frac{\rho_{k+2} - \rho_{k+1}}{X_{k+2}^n - X_{k+1}^n} \right)^2 - \left(\frac{\rho_{k+1} - \rho_k}{X_{k+1}^n - X_k^n} \right)^2}{(\rho_{k+3/2} - \rho_{k+1/2})} \\ & - \frac{\rho_k - \rho_{k-1}}{X_k^n - X_{k-1}^n} \frac{\left(\frac{\rho_{k+1} - \rho_k}{X_{k+1}^n - X_k^n} \right)^2 - \left(\frac{\rho_k - \rho_{k-1}}{X_k^n - X_{k-1}^n} \right)^2}{\rho_{k+1/2} - \rho_{k-1/2}} \Bigg) / (\rho_{k+1} - \rho_k), \end{aligned}$$

and the associated initial condition is

$$X_k^0 = X_0(\rho_k).$$

The boundary conditions (16) are discretized as

$$\begin{aligned} \frac{\rho_{k+1} - \rho_k}{X_{k+1}^n - X_k^n} &= \frac{\rho_k - \rho_{k-1}}{X_k^n - X_{k-1}^n}, \\ X_k^{n+1} &= X_k^n, \end{aligned}$$

which are satisfied for $k = 0, N$ if we choose

$$\begin{aligned} \rho_{-\alpha} &= 2\rho_0 - \rho_\alpha = -\rho_\alpha, \\ \rho_{N-\alpha} &= 2\rho_N - \rho_{N-\alpha} = 2m - \rho_{N-\alpha}, \end{aligned} \tag{23}$$

for $\alpha = 1/2, 1, 3/2, 2$ and

$$\begin{aligned} X_{k-\beta}^n &= 2X_0^n - X_\beta^n, \\ X_{N+\beta}^n &= 2X_N^n - X_{N-\beta}^n, \end{aligned} \tag{24}$$

for $\beta = 1, 2$; we impose this boundary conditions by expanding the physical domain and adding ghost points to each side of the grid.

In order to grant the solvability of (13) we need that the scheme be monotonicity preserving: if we start with a strictly monotone initial datum, it must stay strictly monotone. To prove this property we introduce a splitting for the function ϕ : since it is not monotone we have to choose two sufficently smooth functions ϕ_1 and ϕ_2 such that

$$\phi = \phi_1 - \phi_2 \quad \text{and} \quad \phi_j' \geq 0 \text{ for } j = 1, 2.$$

We also define the Lipschitz constants $L_j = \max_{0,m} \phi_j'$ of ϕ_j; since we are going to show that the scheme is monotonicity preserving if Δt is subjected to a constraint depending on the size of L_j, we must pay attention to choose ϕ_j such that L_j be as small as possible. Let us introduce the following notation

$$\delta v_k^n = v_k^n - v_{k-1}^n;$$

now we are able to prove the following

Theorem 3.1. *Let $X^n_{k+1} - X^n_k \geq \gamma^n > 0$ for each k. Then under the constraint on the time integration step*

$$\frac{2\Delta t}{(\gamma^n)^2} \sup\left\{\frac{\delta\rho_k}{\min\{\delta\rho_{k\pm1/2}\}}\right\}(L_1+L_2)+\frac{4|q|\Delta t}{(\gamma^n)^4}\sup\left\{\frac{\sup\{\delta\rho_k,\delta\rho_{k\pm1}\}}{\inf\{\delta\rho_k,\delta\rho_{k\pm1/2}\}}\right\}\leq 1, \quad (25)$$

we have that $X^{n+1}_{k+1} - X^{n+1}_k > 0$ for each k.

Proof. The expression $X^{n+1}_{k+1} - X^{n+1}_k$ is very length to write in term of X^n_k, so let us introduce

$$Y^n_k = \frac{\delta\rho_{k+2}}{\delta X^n_{k+2}}.$$

First we consider the expression $X^{n+1}_{k+1} - X^{n+1}_k$ for values of k such that no ghost points are involved in the computations: since the new value of X^{+1}_k is derived from the values of X^n and ρ evaluated for (22) $[k-2, k-1, k, k+1, k+2]$, we consider $k = 2, \ldots, N-2$. From (22) we can write

$$\begin{aligned}\delta X^{n+1}_k &= \delta X^n_{k+1} - \frac{\Delta t}{\delta\rho_{k+3/2}}\left(\phi_1\left(Y^n_{k+2}\right) - \phi_1\left(Y^n_{k+1}\right) - \phi_2\left(Y^n_{k+2}\right) + \phi_2\left(Y^n_{k+1}\right)\right)\\ &+\frac{\Delta t}{\delta\rho_{k+1/2}}\left(\phi_1\left(Y^n_{k+1}\right) - \phi_1\left(Y^n_k\right) - \phi_2\left(Y^n_{k+1}\right) + \phi_2\left(Y^n_k\right)\right)\\ &-\frac{q\Delta t}{2\delta\rho_{k+3/2}}\left(\Psi^n_{k+3/2} - \Psi^n_{k+1/2}\right) + \frac{q\Delta t}{2\delta\rho_{k+1/2}}\left(\Psi^n_{k+1/2} - \Psi^n_{k-1/2}\right).\end{aligned}$$

The functions ϕ_1 and ϕ_2 are smooth, so applying the mean value theorem we can find $\xi^n_{j,k+1/2} \in [\min\{Y^n_k, Y^n_{k+1}\}, \max\{Y^n_k, Y^n_{k+1}\}]$ for $j = 1, 2$ such that, setting $\phi'_{j,k+1/2} = \phi'_j(\xi^n_{j,k+1/2})$, the preceding expression becomes

$$\begin{aligned}\delta X^{n+1}_k &= \delta X^n_{k+1} - \frac{\Delta t}{\delta\rho_{k+3/2}}\left(\phi'_{1,k+3/2}\left(Y^n_{k+2} - Y^n_{k+1}\right) - \phi'_{2,k+3/2}\left(Y^n_{k+2} - Y^n_{k+1}\right)\right)\\ &+\frac{\Delta t}{\delta\rho_{k+1/2}}\left(\phi'_{1,k+1/2}\left(Y^n_{k+1} - Y^n_k\right) - \phi'_{2,k+1/2}\left(Y^n_{k+1} - Y^n_k\right)\right)\\ &-\frac{q\Delta t}{2\delta\rho_{k+3/2}}\left(\Psi^n_{k+3/2} - \Psi^n_{k+1/2}\right) + \frac{q\Delta t}{2\delta\rho_{k+1/2}}\left(\Psi^n_{k+1/2} - \Psi^n_{k-1/2}\right),\end{aligned}$$

Remembering the definition of $\Psi^n_{k+1/2}$ and that Y^n_k, X^n_k, ρ_k are positive, we get

$$\begin{aligned}-\Psi^n_{k+1/2} &\geq -\left(Y^n_{k+1}\frac{\left(Y^n_{k+2}\right)^2}{\delta\rho_{k+3/2}} + Y^n_k\frac{\left(Y^n_k\right)^2}{\delta\rho_{k+1/2}}\right)/\delta\rho_{k+1},\\ \Psi^n_{k+1/2} &\geq -\left(Y^n_{k+1}\frac{\left(Y^n_{k+1}\right)^2}{\delta\rho_{k+3/2}} + Y^n_k\frac{\left(Y^n_{k+1}\right)^2}{\delta\rho_{k+1/2}}\right)/\delta\rho_{k+1},\end{aligned}$$

and then, taking into account the previous relations, we have

$$\begin{aligned}\delta X_k^{n+1} \geq\ & \delta X_{k+1}^n - \frac{\Delta t}{\delta\rho_{k+3/2}}\left(\phi'_{1,k+3/2}Y_{k+2}^n + \phi'_{2,k+3/2}Y_{k+1}^n\right)\\ & -\frac{\Delta t}{\delta\rho_{k+1/2}}\left(\phi'_{1,k+1/2}Y_k^n + \phi'_{2,k+1/2}Y_{k+1}^n\right)\\ & +\frac{q\Delta t}{2\delta\rho_{k+3/2}}\left(Y_{k+2}^n\frac{\left(Y_{k+2}^n\right)^2}{\delta\rho_{k+5/2}} + Y_{k+1}^n\frac{\left(Y_{k+2}^n\right)^2}{\delta\rho_{k+3/2}}\right)/\delta\rho_{k+2}\\ & +\frac{q\Delta t}{2\delta\rho_{k+3/2}}\left(Y_{k+1}^n\frac{\left(Y_{k+2}^n\right)^2}{\delta\rho_{k+3/2}} + Y_k^n\frac{\left(Y_k^n\right)^2}{\delta\rho_{k+1/2}}\right)/\delta\rho_{k+1}\\ & +\frac{q\Delta t}{2\delta\rho_{k+1/2}}\left(Y_{k+1}^n\frac{\left(Y_{k+2}^n\right)^2}{\delta\rho_{k+3/2}} + Y_k^n\frac{\left(Y_k^n\right)^2}{\delta\rho_{k+1/2}}\right)/\delta\rho_{k+1}\\ & +\frac{q\Delta t}{2\delta\rho_{k+1/2}}\left(Y_k^n\frac{\left(Y_k^n\right)^2}{\delta\rho_{k+1/2}} + Y_{k-1}^n\frac{\left(Y_k^n\right)^2}{\delta\rho_{k-1/2}}\right)/\delta\rho_k\end{aligned}$$

which is strictly positive under the condition (25).

The last boundary cases of $k = 0, 1, N-2, N-1$ can be treated in a similar manner remembering (23) and (24) and the positivity is preserved under the same condition. □

Remark 1. The time integration is explicit and so the time step restriction Δt reflects the fact that the equation includes both second and fourth order terms: for small values of the surface tension constant q and with relatively few points of approximation the condition (25) reduces to

$$\Delta t \leq C_1 \inf_k\{X_{k+1}^n - X_k^n\}^2$$

as the parabolic nature of the numerical scheme is the dominant one. When q is determining or we have a greater number of grid points, the constraint becomes the more restrictive one

$$\Delta t \leq C_2 \inf_k\{X_{k+1}^n - X_k^n\}^4$$

showing the fourth order nature of the equation. The last inequality can be very constrictive on the size of Δt : to avoid this an implicit time integration, like Crank-Nicholson or Backward Euler, can be used.

Moreover, the previous theorem is not enough to assure the convergence of the numerical scheme and does not avoid that the time step Δt becomes more and more small. We show through several numerical simulations that $\delta X_k^n \geq a > 0$ for $n = 1, \ldots,$ testing empirically the stability and the convergence of the algorythm. We postpone to a future work the complete analysis of the scheme and the investigation of implicit time integrators.

4. **Numerical tests.** In this section we present several numerical tests to show the behaviour of the numerical scheme (22) in different situations: in each one we use $N = 125$ spatial grid points and the time step Δt is chosen in accordance with (25). For all the simulations we performed we found that the value of $\inf\{X_{k+1}^n - X_k^n\}$ for each $n > 0$ is bounded between 0.5 and 0.64, and this allows the scheme to proceed in time without stopping as noticed in remark 1.

The simulations are organized as follows: in the first set we evolve a symmetric initial datum with different values of the surface tension q to show how the spatial patterns change varying the interfacial energy. In the second set of simulations we

use an unsymmetrical initial datum and we investigate the final states reached with different choiches of q : in particular we focus our attention on the attainment of a "stable" final state consisting in just two regions with different concentrations. The last simulation inspects the behaviour of the scheme in the presence of an highly perturbed initial datum. Each simulation comes with the computation of the discrete energy, which is obtained approximating the energy integral (17) using the solution X_k^n given by the scheme.

In the first set of tests we start from the initial datum

$$u_0(x) = \frac{1}{2}\cos(2\pi x) + \frac{3}{2} \quad x \in [0,1] \tag{26}$$

and we consider $q = -10^{-4}, -5 \cdot 10^{-4}, -10^{-3}$ as values of the surface tension q. Figure 1 is obtained with the smallest parameter in absolute value, $q = -10^{-4}$: this reflects on the spatial patterns, which are very fine, expecially in the first phase of the simulations. Some of the alternated regions of different phases tend to collate as time increases, resulting in a final state which consists of four regions with concentration $u = 2$ spaced out by three regions with concentration $u = 1$.

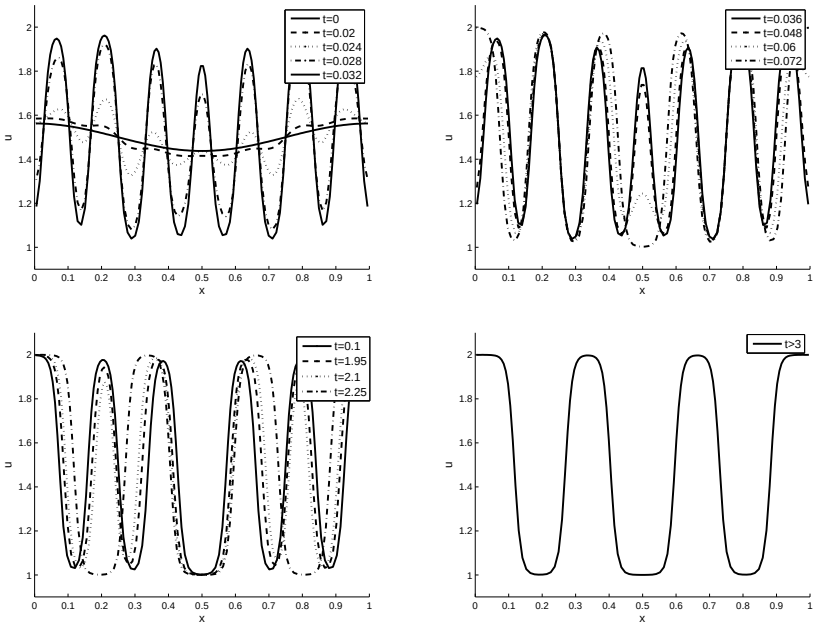

FIGURE 1. The evolution of a cosine function with a small value of the surface tension ($q = -10^{-4}$): at the beginnning several alternated regions arises, some of which tend to collate, while the final state consists in the alternance of seven regions.

In the second simulation we increase the absolute value of q to $-5 \cdot 10^{-4}$: the behaviour of u is quite different, since initially we have a lower number of separated regions which collate towards a stable state with just three regions, as shown in figure **??**. Morevoer, the overall process is faster.

In the last simulation with inital datum (26) we set $q = -10^{-3}$: the process is very similar to the previous one, the main difference is that the separation of

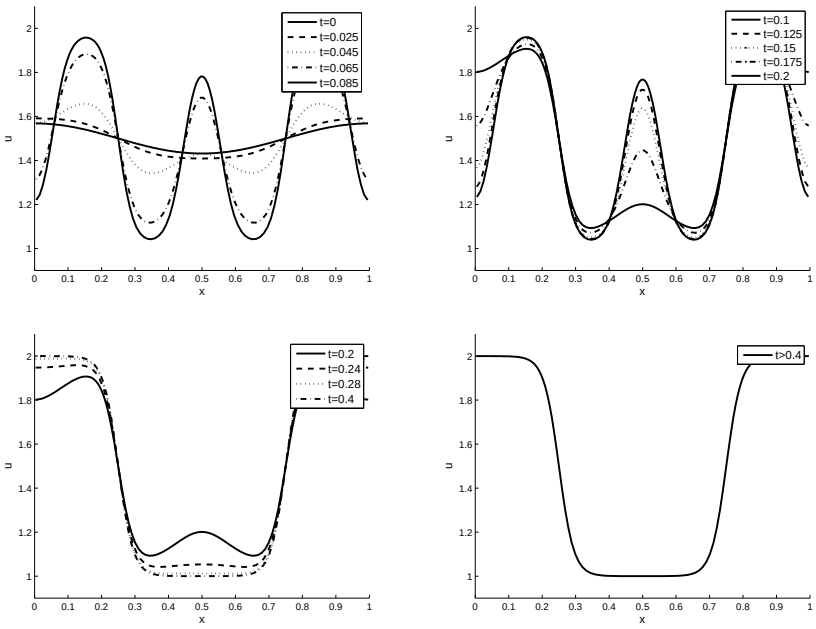

FIGURE 2. The evolution of a cosine function with an intermediate value of the surface tension ($q = -5 \cdot 10^{-4}$): the number of separated regions is lower then in figure 1 and the overall process is faster.

the phases is even more fast and that the interface between the different regions is a bit larger. We remark that the initial symmetry of (26) is preserved by the scheme during all the simulation and that this prevents the organization of the concentration in just two regions.

Finally in figure 4 we show that, for the first set of simultations, the proposed scheme preserves at the discrete level the energy dissipation property (18).

In the next set of simulations we start from a more oscillating initial datum

$$u_0(x) = (0.1\sin(2\pi x) + 0.01\cos(4\pi x) + 0.06\sin(4\pi x) + 0.02\cos(10\pi x)) + 1.5 \quad (27)$$

like in [7, 8]; the potential function Φ used by Furihata and Ye is different form that we used and so the results could be compared only after an affine transformation.

This time the inital datum (27) is non-symmetric, so we could expect a final state constituted by two regions. Again we test several values of the parameter: in the first simulation shown in figure 5, we set the surface tension to $q = -2 \cdot 10^{-4}$, and we can see that the weak interfacial energy coupled with the presence of the oscillations, induces the formation of several regions with alternated concentrations which takes more time to settle down. The final state again consists of more than two regions.

A monotone final state consisting of only two regions can be observed in figures 6 and 7, which correspond respectively to the choiche of $q = -5 \cdot 10^{-4}$ and $q = -1 \cdot 10^{-3}$: the two simulations differ essentially in the time needed to attain the final state, which appears for much smaller times in the case of the stronger interfacial energy induced by $q = -1 \cdot 10^{-3}$.

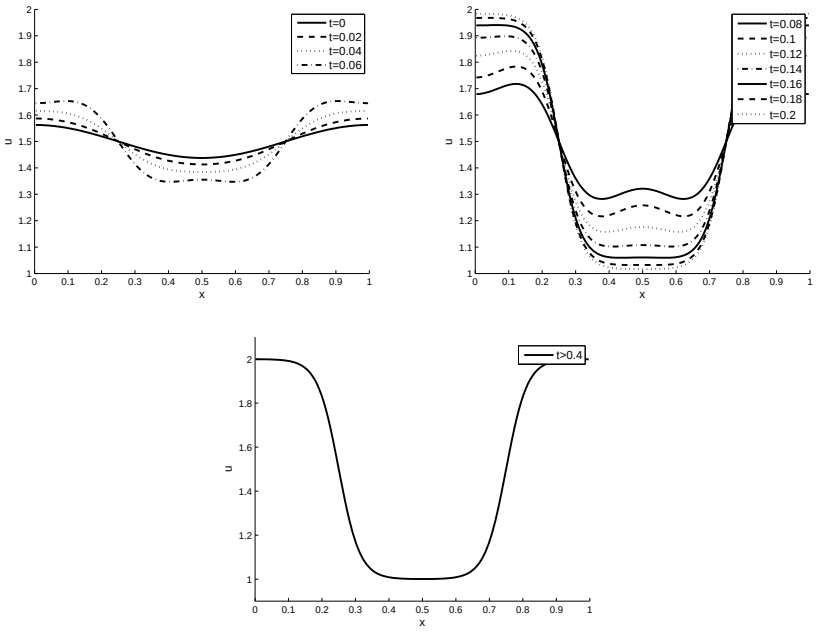

FIGURE 3. The evolution of a cosine function with an high value of the surface tension ($q = -10^{-3}$) the process is very similar to that with $q = -5 \cdot 10^{-4}$, but it is faster with larger interfaces.

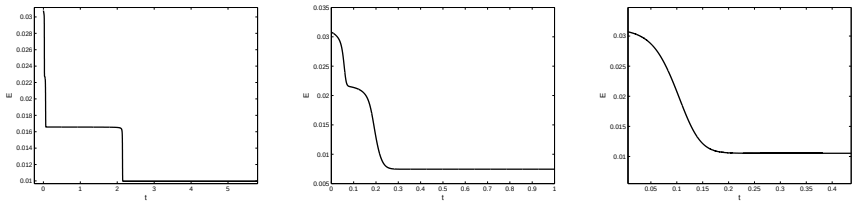

FIGURE 4. The discrete energy for the evolution of the cosine function (26) with different values of q. The computation is carried on until E is essentially constant.

The last figures 8 show that also in this case the discrete energy dissipates.

In the last test we perturb randomly the starting state (27): even with a small value of $q = -10^{-4}$ the original unevenness is fastly smoothed out at the very initial time (see figure 10), then the process is carried out as in the previous situations.

In figure 10 we show that also in this situation the proposed numerical scheme grants the dissipation of energy at the discrete level.

The last test we performe is devoted to investigate numerically the convergence of the scheme. Since we used a Wasserstein approach to the study of the Cahn-Hilliard equation it seems natural to test the convergence of the numerical approximation in the Wasserstein p-metric, which, through the pseudo-inverse, rewrites as

$$W_p(u^n, u) = \int_0^1 (X^n(\rho))$$

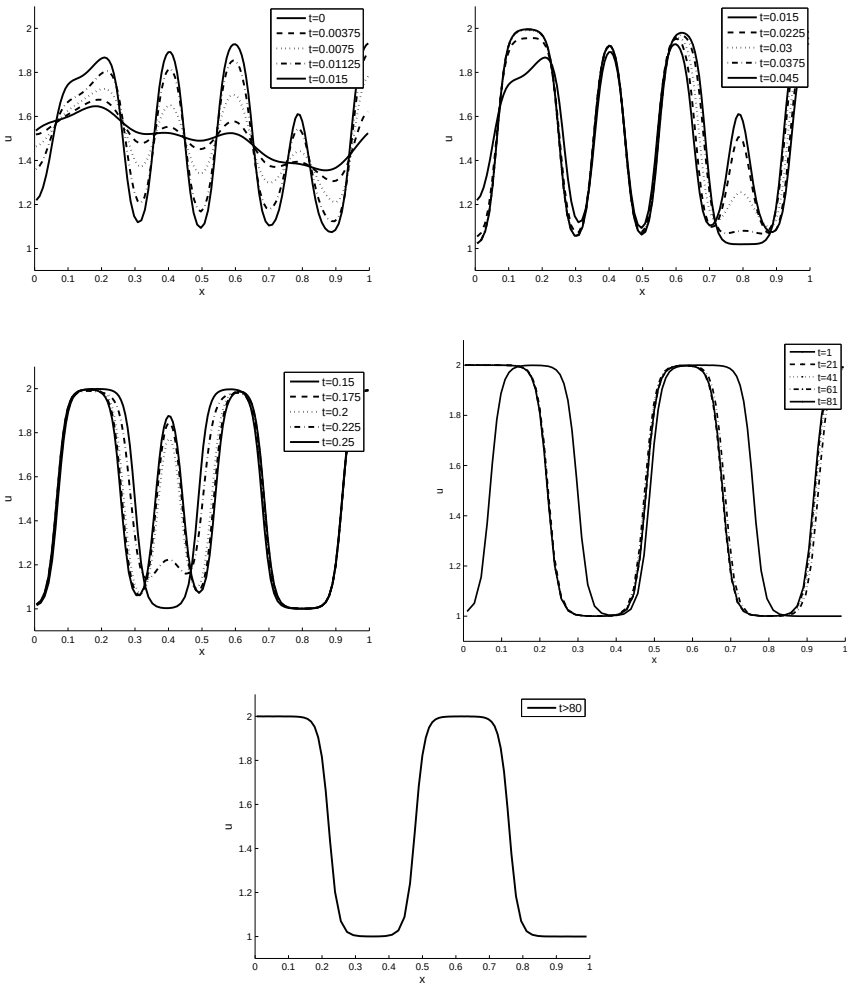

FIGURE 5. The evolution of the non-symmetric and oscillating initial datum (27): with the surface tension set to $q = -2 \cdot 10^{-4}$ the final state is reached within time longer than the simulations starting with the cosine.

: we recall tuse (26) as initial state and computing the solution at time $t = 0.4$, when the phase separation already occoured. The reference solution is computer using a fine grid: since the values of ρ_k does not match on different grids due to the non-uniformity of the spatial subdivision, we must interpolate on the coarse grid to obtain the values of X_k for the same values of $\{\rho_k\}$; the integral is computed using a quadrature formula. The results are reported in table 1, where we test the convergence in norm ... and we obtain a second order convergence rate in both norms.

5. **Conclusions.** Analisi, schema implicito

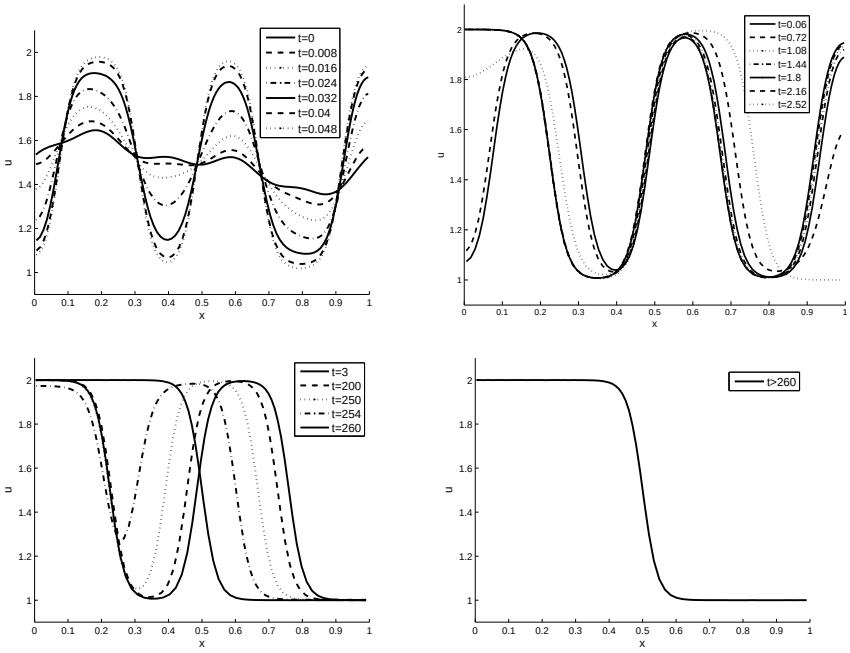

FIGURE 6. The evolution of the non-symmetric and oscillating initial datum (27): with an intermediate value of surface tension $q = -5 \cdot 10^{-4}$ a two phase separated final state is reached after a long time.

N	error	rate	error	rate
15	1.137e-03		1.148e-3	
30	1.850e-04	2.620	2.887e-04	1.991
60	4.247e-05	2.122	6.523e-05	2.146
120	8.525e-06	2.316	1.275e-05	2.354

TABLE 1. Convergence test in norm ...

6. **Cose da aggiungere.** Specificare dove necessario gli spazi a cui appartengono le funzioni
Specificare come si scelgono i valori $k + 1/2$
Dire che si verifica numericamente che l'energia decresce
Uniformare: pseudo-inverse o pseudo inverse
Aggiungere splitting esplcito per *phi*?

REFERENCES

[1] Paul C. Fife, *Models for phase separation and their mathematics*, Electronic Journal of Differential Equations, **48** (2000), 1–26.
[2] J. W. Cahn, *Theory of crystal growth and interface motion in crystalline materials*, Acta Metallurgica, **48** (1960), 554–562.
[3] J. W. Cahn, *On spinodal decomposition*, Acta Metallurgica, **9** (1961), 795–801.

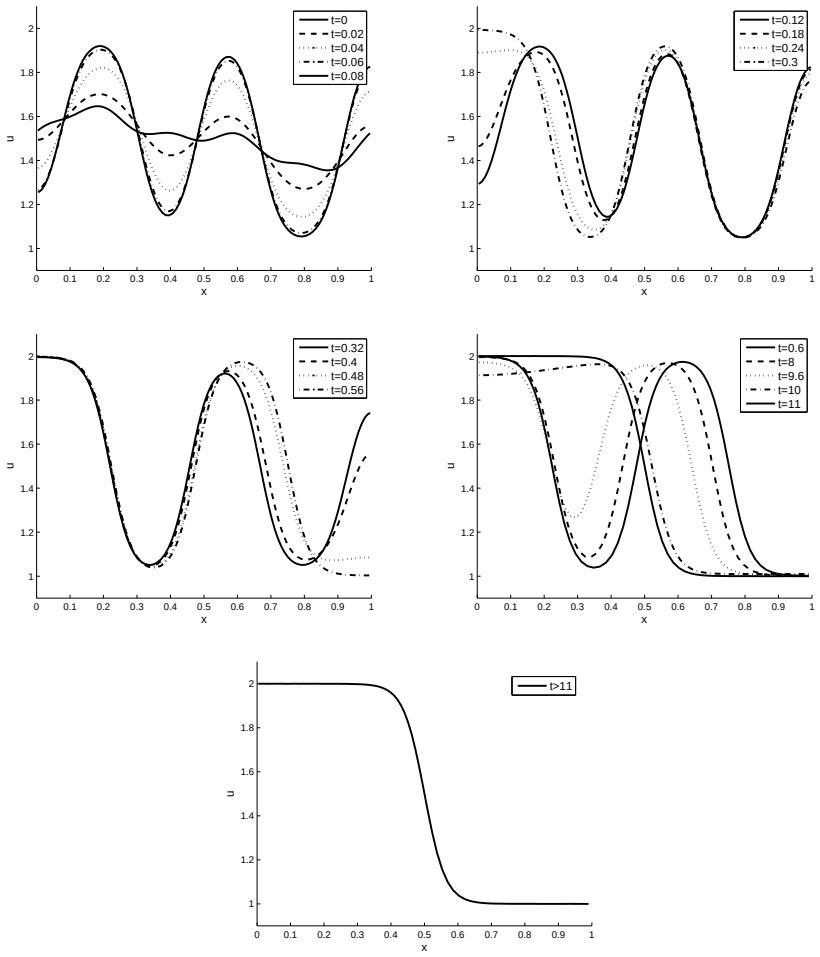

FIGURE 7. The evolution of an oscillating intial datum: with an high absolute value of surface tension ($q = 1 \cdot 10^{-3}$) the final state is reached at an earlier time.

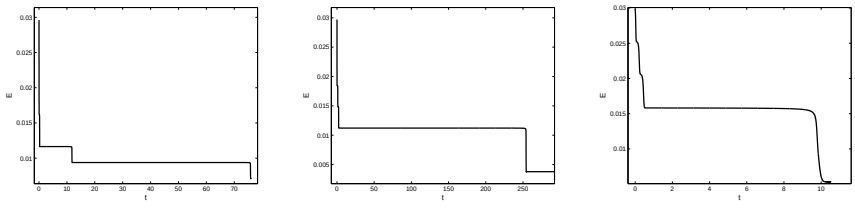

FIGURE 8. The discrete energy for the evolution of function (27) with different values of q. The computation is carried on until E is essentially constant.

[4] J. W. Cahn, *On spinodal decomposition in cubic crystals*, Acta Metallurgica, **10** (1962), 179–183.

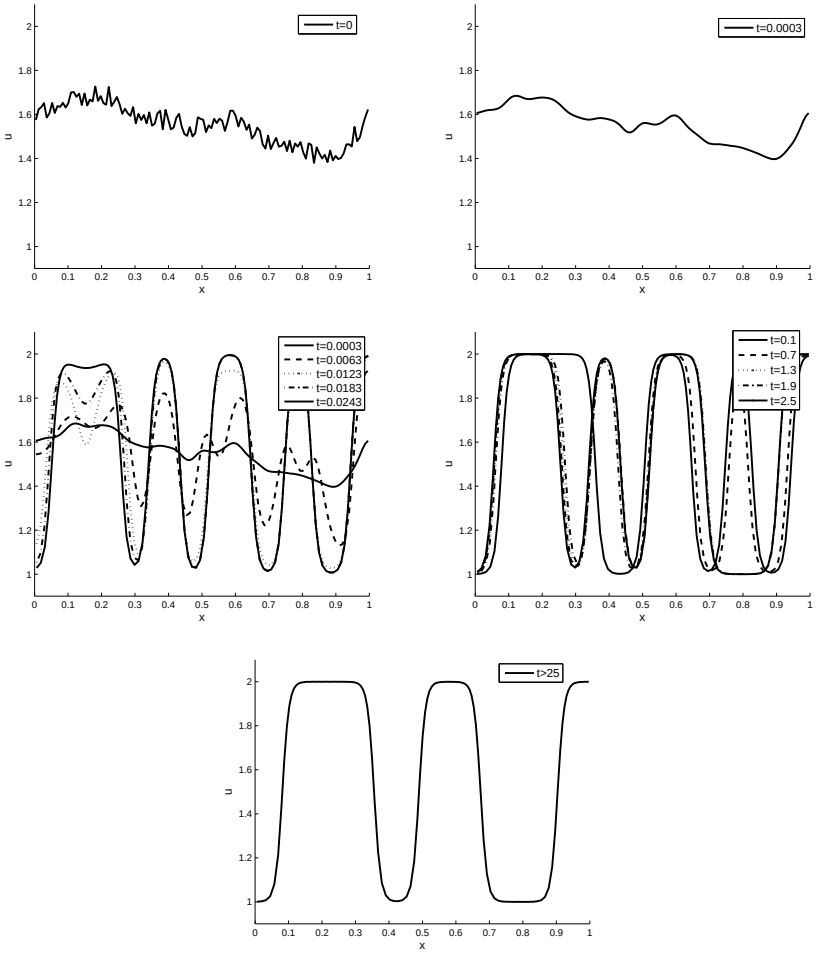

FIGURE 9. The evolution of an oscillating perturbed initial datum: even with $q = -10^{-4}$ the solution is quickly smoothed out.

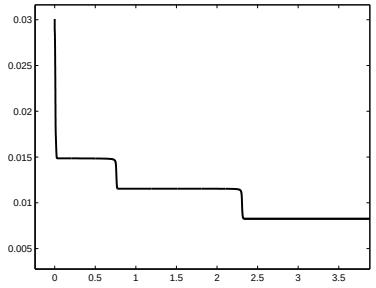

FIGURE 10. The discrete energy for the evolution of a perturbation of the function (27). The computation is carried on until E is essentially constant.

[5] J. W. Cahn, *Phase separation by spinodal decomposition in isotropic systems*, J. Chem. Physics, **42** (1965), 93–99.
[6] J. W. Cahn and J. E. Hilliard, *Free energy of a nonuniform system I. Interfacial free energy*, J. Chem. Phys. **28** (1958), 258–267.
[7] D. Furihata, *A stable and conservative finite difference scheme for the Cahn-Hilliard equation*, Numer. Math. **87** (2001), 675–699
[8] X. Ye, *The Legendre collocation method for the Cahn-Hilliard equation*, J. Comput. Appl. Math. **150** (2003) 87–108

Received xxxx 20xx; revised xxxx 20xx.

E-mail address: fausto.cavalli@ing.unibs.it
E-mail address: giovanni.naldi@unimi.it